Fundamental Research 1 (2021) 393–398

Contents lists available at ScienceDirect

Fundamental Research

journal homepage: http://www.keaipublishing.com/en/journals/fundamental-research/

Article

Ion–solvent chemistry in lithium battery electrolytes: From mono-solvent to multi-solvent complexes

Xiang Chen[1], Nan Yao[1], Bo-Shen Zeng, Qiang Zhang*

Beijing Key Laboratory of Green Chemical Reaction Engineering and Technology, Department of Chemical Engineering, Tsinghua University, Beijing 100084, China

ARTICLE INFO

Article history:
Received 10 May 2021
Received in revised form 22 May 2021
Accepted 7 June 2021
Available online 30 June 2021

Keywords:
Lithium batteries
Ion–solvent complexes
Electrolyte solvation
Electrolyte stability
Density functional theory calculations
Molecular dynamics simulations

ABSTRACT

The building of safe and high energy-density lithium batteries is strongly dependent on the electrochemical performance of working electrolytes, in which ion–solvent interactions play a vital role. Herein, the ion–solvent chemistry is developed from mono-solvent to multi-solvent complexes to probe the solvation structure and the redox stability of practical electrolytes. The decrease in energies of the highest occupied molecular orbital (HOMO) and the lowest unoccupied molecular orbital (LUMO) of solvents in lithium-ion solvation shells becomes less significant as the number of coordinated solvents increases, but both the HOMO and LUMO energies of the coordinated solvents remain lower than those of free solvents. A positive and approximately linear relationship was found between the decrease in the HOMO/LUMO energy and the average binding energy between Li^+ and the coordinated solvents. A binary-solvent complex model further highlight the significant importance of the electrolyte solvation environment in regulating electrolyte stability, and it is essential to consider electrolyte stability from the perspective of ion–solvent complexes. These fresh insights into the energy chemistry of multi-solvent complexes provide critical references for electrolyte design and cell optimization.

1. Introduction

To build a renewable energy system and achieve the goal of carbon neutrality, high-performance energy storage devices are urgently required everywhere from personal energy usage to large-scale smart grids [1–3]. Lithium batteries (LBs) with a promising energy density and long cycling lifespan are widely applied in our daily life and are consequently considered to reconstruct future energy systems [4–6]. However, future energy systems require extremely strict demands for next-generation LB technologies, such as safety, high- or low-temperature performance, rate performance, and recycling [7–10].

To meet the increasing demands of future energy systems and build promising next-generation LBs, high-performance electrolytes are indispensable and play a vital role in stabilizing the interfaces between electrolytes and high-activity electrodes [11–15]. Compared with graphite anodes used in commercial lithium-ion batteries, high-capacity electrodes such as lithium metal anodes generally induce much more serious interfacial reactions and cause faster electrolyte degradation and capacity decay. Most organic solvents are unstable with lithium metal anodes, and decompose to produce flammable gases, such as methane and ethylene [16]. The exhaustion of electrolytes not only induces rapid capacity degradation and short cycling of batteries but also causes safety hazards. Therefore, routine organic electrolytes are facing significant challenges in stabilizing the electrolyte–electrode interface in high-energy-density LBs, and therefore new electrolytes are urgently required [17–19].

To construct highly stable electrolytes for constructing high-energy-density LBs, many solvents, lithium salts, and additives have been developed through trial and error [14,20–22]. However, a deep understanding of the fundamental interactions in electrolytes and a rational strategy for the design of electrolytes are lacking. Recently, an ion–solvent complex model was proposed to probe electrolyte component interactions and redox stabilities and provide new insights into electrolyte design [23–25]. Specifically, the energy level of the lowest unoccupied molecular orbital (LUMO) of the solvents can be significantly decreased by the coordinated lithium ions. As a result, the solvents in lithium-ion solvation shells preferentially decompose on lithium metal anodes compared to free solvents. The ion–solvent chemistry has inspired a new electrolyte design strategy for cation additives and has achieved great applications in sodium metal batteries [26].

Although the ion–solvent complex model is well established to probe the electrolyte stability and afford rational strategies for electrolyte design, only a mono solvent in lithium-ion solvation shells was previously considered. In practical electrolytes, lithium ions are solvated by several solvents, and the solvent–solvent interactions cannot be neglected. A model of ion–multi-solvent complexes should be further explored to probe electrolyte stability, from which the electrolyte solvation structure and redox stability can be well understood at the atomic level. Fur-

* Corresponding author.
E-mail address: zhang-qiang@mails.tsinghua.edu.cn (Q. Zhang).
[1] Xiang Chen and Nan Yao contributed equally to this work.

https://doi.org/10.1016/j.fmre.2021.06.011

thermore, by combining ion–solvent chemistry with machine learning methods, it is expected that a rational electrolyte design will accelerate the development of next-generation LBs [11].

In this study, ion–solvent chemistry was developed from mono-solvent to multi-solvent models through both molecular dynamics (MD) simulations and density functional theory (DFT) calculations. Generally, the energies of the HOMO and LUMO of solvents in a solvation shell are lower than that of free solvents, indicating the reduced reductive stability and the enhanced oxidative stability of coordinated solvents regardless of their number. Additionally, a positive and approximately linear relationship was found between the decrease in the HOMO/LUMO energy and the average binding energy. As a result, the decrease in the HOMO and LUMO energies becomes less significant when the number of coordinated solvents increases. In addition, both the solvent type and solvation environment are equally important in regulating solvent stability, which provides new insights into electrolyte design.

2. Computational details

Molecular dynamics (MD) simulations: MD simulations were conducted using the large-scale atomic/molecular massively parallel simulator (LAMMPS) code [27]. The solvent force field parameters were generated by the LigParGen web server [28] except for the atomic charge of restrained electrostatic potential (RESP) atomic partial charges, which were obtained based on electrostatic potential (ESP) charges using the Multiwfn program [29]. The parameters for Li^+ and PF_6^- were obtained from the findings of Jensen *et al.* [30] and Doherty *et al.* [31], respectively. A cutoff of 12 Å was used for both the van der Waals interactions and the long-range correction (particle–particle particle-mesh) of Coulombic interactions. The time step was set to 1 fs. All systems were first equilibrated in the NPT ensemble using the Parrinello–Rahman barostat [32] for 2 ns to maintain a temperature of 298 K and a pressure of 1 atm with a time constant of 0.1 and 1 ps, respectively. Subsequently, the models were heated from 298 to 350 K in 1.0 ns and were maintained at 350 K for 1 ns, followed by annealing from 350 to 298 K in 1.0 ns and equilibrated at 298 K in an NPT ensemble for another 1 ns. Finally, a production run of 15 ns was conducted at 298 K in the NVT ensemble under a Nose–Hoover thermostat [33,34]. The last 5 ns of the NVT simulations were output every 1000 steps and used for the statistical analysis of solvation structures.

Density functional theory calculations: DFT calculations were conducted in the Gaussian (G09) [35] program with Becke's three-parameter hybrid method using the Lee–Yang–Parr correlation functional (B3LYP) [36]. The solvation effect was considered using the universal solvation model of SMD [37]. Frequency analysis was performed to determine the ground states of the optimized ion–solvent complexes. Two series bases, 6-311++G(d, p) and 6-31G(d, p), were considered. 1,2-dimethoxyethane (DME) was used as an example to check the reliability of the low-accuracy basis, and the results from the two bases agree with each other (Fig. S1 and S2). However, 6-311++G(d, p) cannot be used for the calculation of the lithium-ion solvation shell with six solvents. Therefore, the 6-31G(d, p) basis was used while considering the number of coordinated solvents, and the 6-311++G(d, p) basis was adopted in both the binary solvent systems and the calculation of ESP charges of solvent atoms according to the Merz–Singh–Kollman scheme [38,39]. The binding energy (E_b) between a lithium ion and a solvent is defined as follows:

$$E_b = E_{Complex} - E_{Li} - E_{Solvents} \quad (1)$$

where $E_{Complex}$ is the total energy of the cation–solvent complex, E_{Li} the total energy of Li^+, and $E_{solvents}$ the sum of the total energy of each solvent in the complex. It should be noted that the interaction between solvents is included in the as-defined binding energy.

3. Results and discussion

Widely used electrolyte solvents, including ethylene carbonate (EC), diethyl carbonate (DEC), dimethyl carbonate (DMC), fluoroethylene carbonate (FEC), 1,3-dioxolane (DOL), and DME were considered in this work. Li salts can be dissolved in these solvents to form ion–solvent complexes, which are key components in probing electrolyte decomposition on Li metal anodes. To determine the solvation structures in the electrolytes, MD simulations were first conducted, and 1.0 M lithium hexafluorophosphate ($LiPF_6$) was introduced (Fig. 1 and S3). Generally, lithium ions are directly bound to the oxygen atoms in solvents, or to the fluorine atoms in PF_6^- anions, and have a coordination number of five to six in all solvents (Fig. S3).

However, the distribution of the number of coordinated solvents (NCS) in lithium-ion solvation shells varies significantly for different solvents because of their distinguishing solvating abilities (Fig. 1). The cyclic esters EC and FEC exhibit a similar coordination structure, with an NCS ranging from four to six, and an NCS of five is predominant (Fig. 1(a) and 1(d)). In particular, 91.3% of the Li ions are coordinated with five EC molecules, and the average NCS is 4.95 in the EC electrolytes. The average NCS is 5.28 for the FEC electrolytes with five and six FEC solvents in Li^+ solvation shells, accounting for 62.2% and 31.3%, respectively, showing a stronger coordination ability of FEC than EC. Compared with EC and FEC, linear ester DEC and DMC have smaller NCSs ranging from three to five, and an NCS of four is predominant (Fig. 1(b) and 1(c)). The average NCS is 3.89 and 4.44 for DEC and DMC, respectively, which can be explained by the larger steric hindrance of linear molecules than that of cyclic molecules. In addition, compared with DEC, the molecular chain of DMC is shorter, and DMC consequently delivers a larger average NCS.

The conditions of ether DOL and DME are different from those of the ester electrolytes (Fig. 1(e) and 1(f)). The NCS distribution of DOL is very wide, ranging from zero to five, which is caused by the weak interaction between Li ions and DOL molecules. As a result, a large amount of PF_6^- was introduced into the lithium-ion solvation shell. Specifically, the coordination numbers are 1.93 and 3.88 for DOL and PF_6^-, respectively. In contrast, DME possesses a very large binding energy with Li ions because the two oxygen atoms in the DME molecule can interact with one lithium ion simultaneously. As a result, 100% of the Li ions are coordinated with three DME molecules.

As discussed above, lithium ions are generally solvated by more than one solvent, while any previous ion–solvent chemistry was established based on a mono-solvent model. In this part, a lithium ion is allowed to interact with several solvents simultaneously to determine the largest NCS in the lithium-ion solvation shell, and the HOMO/LUMO energy and the evolution of binding energy with the change in NCS were further probed (Fig. 2 and S4). The largest NCS values for DME, DEC, DMC, EC, FEC, and DOL were determined to be 3, 4, 4, 4, 5, and 6, respectively. The corresponding geometrical structures with the largest NCS are shown in Fig. 2(a). Taking the Li^+–EC complex as an example, the Li–O distances in the optimized Li^+–$(EC)_5$ complex are 1.946, 1.957, 1.950, 1.968, and 3.617 Å (Fig. S5). Besides, the binding energy increases slightly from −3.02 to −3.16 eV when an additional EC molecule is introduced into the Li^+–$(EC)_4$ complex, which is mainly attributed to the contribution from solvent–solvent interactions. Therefore, lithium ions can interact with a maximum of four EC molecules. The largest NCS of the other solvents was determined accordingly.

The large binding energy between EC and Li ions is beneficial for forming a stable oxygen tetrahedron in which a Li ion is located in the center, and an extra EC is impeded from the tetrahedron. DEC and DMC molecules have even larger binding energies with Li ions than EC (Fig. 2(b)) and deliver the largest NCS of four. Although the fluorine atom in FEC could withdraw electrons from carbonyl oxygen and is therefore expected to weaken the interaction between a Li ion and FEC molecules, a Li ion can interact with a maximum of five FEC molecules (Fig. S6(a)). An additional FEC is able to break the tetrahe-

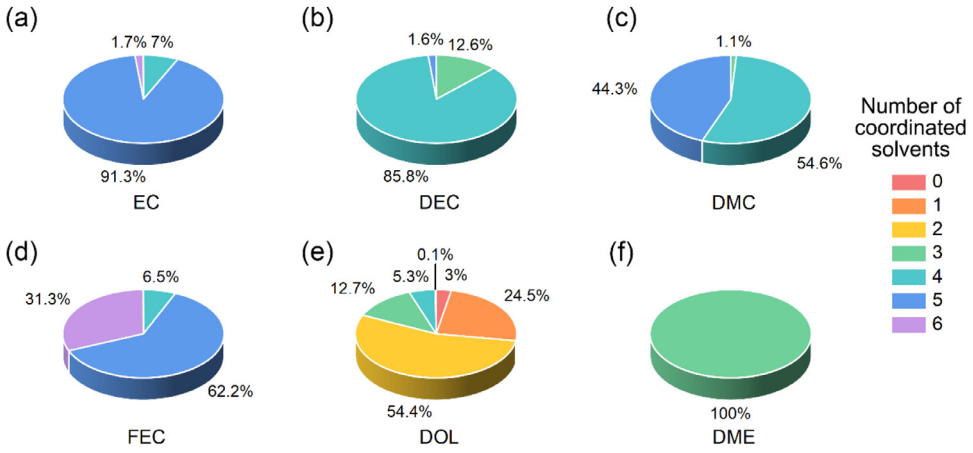

Fig. 1. Statistical analysis of the number of coordinated solvents in lithium ion solvation shells. (a) 1.0 M $LiPF_6$ EC. (b) 1.0 M $LiPF_6$ DEC. (c) 1.0 M $LiPF_6$ DMC. (d) 1.0 M $LiPF_6$ FEC. (e) 1.0 M $LiPF_6$ DOL. (f) 1.0 M $LiPF_6$ DME.

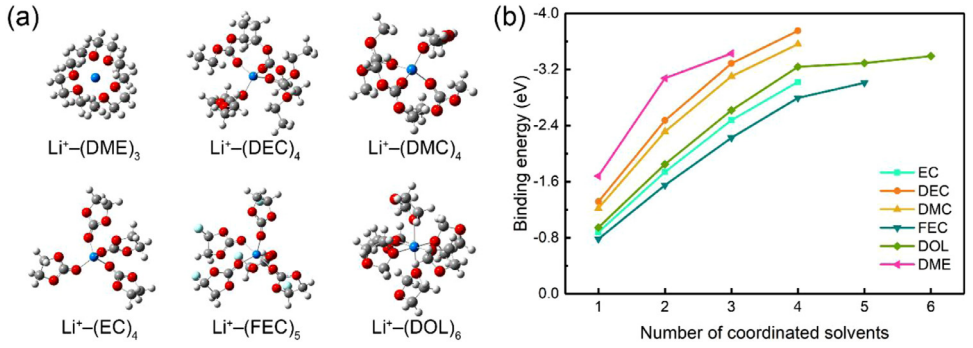

Fig. 2. Geometrical structure and binding energy between a lithium ion and solvents. (a) The geometrical structure of Li^+–$(solvent)_n$ complexes, where n is the number of solvents. Hydrogen, lithium, carbon, oxygen, and fluorine atoms are marked with white, blue, grey, red, and cyan, respectively. (b) The relationship between the binding energy and the number of coordinated solvents in Li^+–$(solvent)_n$ complexes.

dron because of the relatively weaker interaction between the Li ion and FEC molecules and the relatively stronger interaction between FEC molecules [40]. However, lithium ions perfer four coordination when six FEC molecules are simultaneously introduced (Fig. S6(b)). Similarly, DOL molecules possess both a weak interaction with Li ions and little steric hindrance, and consequently deliver a maximum NCS of six.

The largest NCS from DFT calculations agrees with the majority of NCS distribution from MD simulations in FEC, DME, DMC, and DEC electrolytes, as cation–solvent interactions are much stronger than cation–anion interactions in these solvents during MD simulations. The disagreement in DOL electrolytes is induced by the coordination competition between solvents and anions with lithium ions, which is not considered in DFT calculations. Additionally, salt concentration has an obvious influence on the solvation structure, where contact ion pairs and aggregates are preferentially formed in high-concentration electrolytes [41–43]. Therefore, it is reasonable to observe PF_6^- anions in the solvation shell of lithium ions and the discrepancy between the largest NCS obtained from DFT and the majority of the NCS distribution from MD simulations.

The HOMO and LUMO energies were comprehensively compared to probe the redox stability of the multi-solvent complexes (Fig. 3 and S7–S13). All solvents in ion–solvent complexes exhibit decreased HOMO and LUMO energies ranging from −0.6 to −3.2 eV compared with the corresponding free solvents, indicating enhanced oxidative and decreased reductive stability, respectively. Additionally, the change in the redox stability is independent of the number of coordinated solvents. Therefore, the previous conclusion that the formation of ion–solvent complexes promotes electrolyte decomposition on anodes is applicable to multi-solvent conditions, demonstrating the universality of ion–solvent models [23,24].

As the NCS increases, the decrease in the HOMO and LUMO energies becomes less significant. For example, the LUMO energy of EC is reduced by −1.49, −1.41, −1.18, and −0.88 eV in Li^+–EC, Li^+–$(EC)_2$, Li^+–$(EC)_3$, and Li^+–$(EC)_4$ complexes, respectively (Fig. 3(a)). LUMOs consist of carbon and oxygen 2p orbitals of the carbonyl functional group in EC (Fig. S8). The strong electron-withdrawing effect of Li ions reduces the electron density on the oxygen atoms and consequently reduces both the HOMO and LUMO energies. When more EC solvents are introduced into the complex, the electron-withdrawing effect of Li ions on each EC solvent is significantly weakened, and the decrease in the HOMO and LUMO energies becomes less obvious, which agrees with the decrease in the average binding energy between the Li ion and each solvent (Fig. 2(b)). The influence of Li ions on other solvents is similar to that of EC.

The decrease in the HOMO and LUMO energies is further correlated with the average binding energy to understand the chemical origin of the abovementioned phenomena (Fig. 3(e) and 3(f)). As expected, as more solvents enter the lithium-ion solvation shell, the average binding energy decreases, and the decrease in the HOMO and LUMO energies is correspondingly less obvious. A good linear relationship between the HOMO/LUMO energy change and the average binding energy in ester solvents is observed, which is similar to the trend observed for mono-solvent complexes [24]. The Li–$(DOL)_n$ complexes exhibit two linear regions, indicating a change in the interaction between Li ions and DOL molecules. In addition, it is expected that the correlation between the binding energy and the decrease in the HOMO/LUMO energy is useful

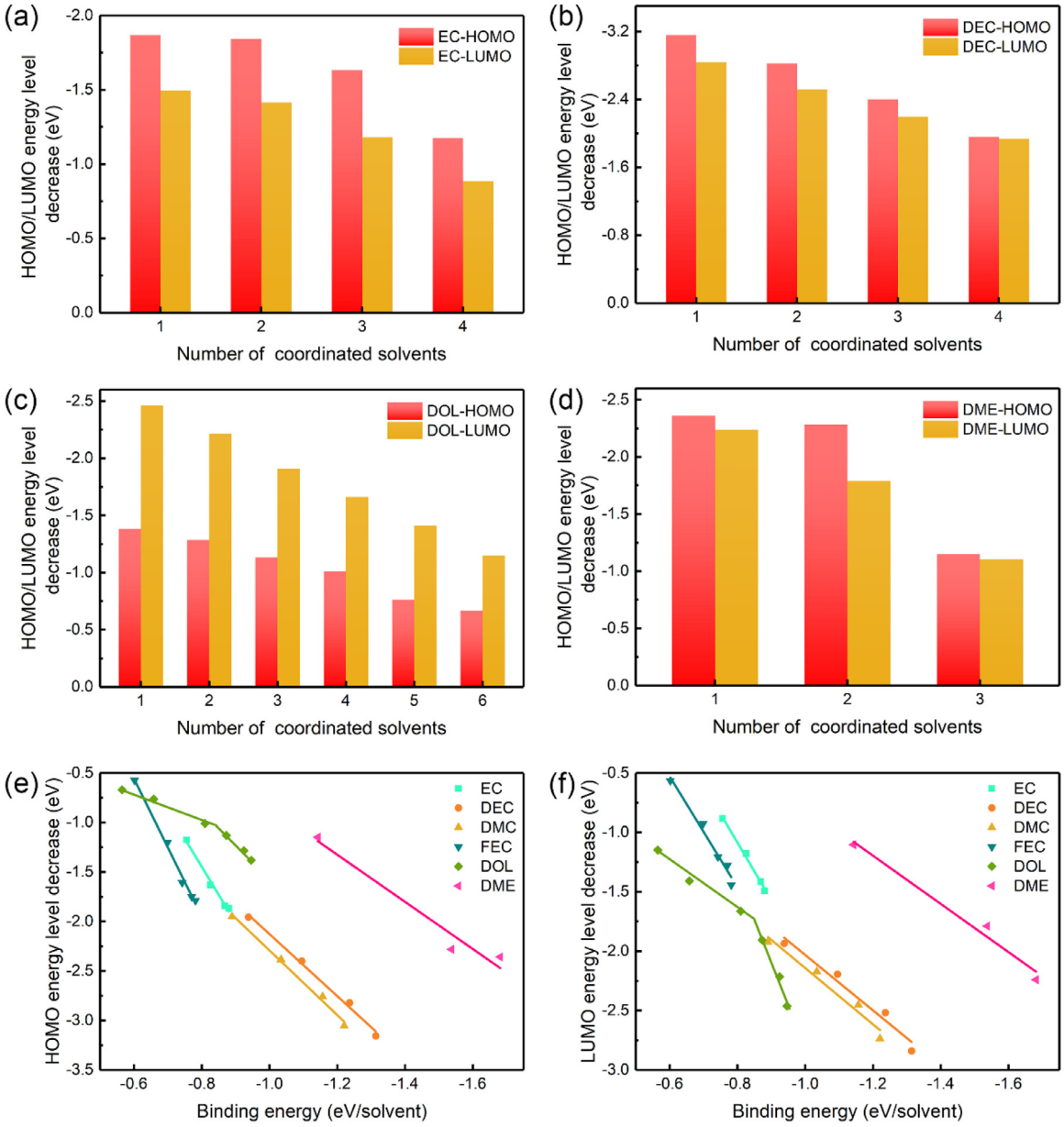

Fig. 3. Summary of the HOMO and LUMO energies of ion–solvent complexes. A comparison of the decrease in HOMO and LUMO energies in (a) Li^+–$(EC)_n$, (b) Li^+–$(DEC)_n$, (c) Li^+–$(DOL)_n$, and (d) Li^+–$(DME)_n$ complexes. The correlation of average binding energy with the decrease in (e) HOMO and (f) LUMO energies.

in understanding the molecular interactions in multi-solvent complexes. The binding energy between a Li ion and each solvent is very difficult to obtain owing to the strongly coupled solvent–solvent interactions. However, it is very convenient to acquire the HOMO and LUMO energies of each solvent, from which the interaction strength can be inferred based on the scaling relationship.

Electrolytes are often composed of more than one type of solvent, and a lithium ion can interact with two different solvent molecules simultaneously. For example, EC–DEC and DOL–DME mixtures are widely used in lithium-ion batteries and lithium–sulfur batteries, respectively [14,44–47]. Therefore, a binary-solvent complex model was further considered, including Li^+–EC–DEC, Li^+–EC–DOL, Li^+–EC–DME, Li^+–DEC–DOL, Li^+–DEC–DME, and Li^+–DOL–DME complexes (Fig. 4 and S14). Three solvation parameters were considered for each binary-solvent complex. Taking the Li^+–EC–DEC complex as an example, the solvation parameters of EC, DEC, and their average values were adopted to model the electrolyte environment. Generally, a larger dielectric constant in the solvation model induces a weaker Li^+–solvent interaction. As a result, a more obvious decrease in the HOMO and LUMO energies was observed in the solvation model with a smaller dielectric constant, indicating the significance of regulating the electrolyte solvation environment.

Under a specific solvation model, the interaction between Li ions and different solvents varies significantly. First, DME possesses the largest binding energy with a Li ion, and the degree of both HOMO and LUMO energies is always higher than that of other solvents in binary-solvent complexes, supporting the correlation between the average binding energy and the decrease in both HOMO and LUMO energies (Fig. 2(b), 3(e), and 3(f)). In particular, DME possesses higher and lower HOMO and LUMO energies than DOL in free solvent and in Li^+–DME–DOL complexes, respectively. In contrast, DOL exhibits the smallest HOMO and LUMO energy decrease, agreeing with the experimental cognition that ester solvents generally possess a stronger dissolving ability toward lithium salts and a larger binding energy with lithium ions than

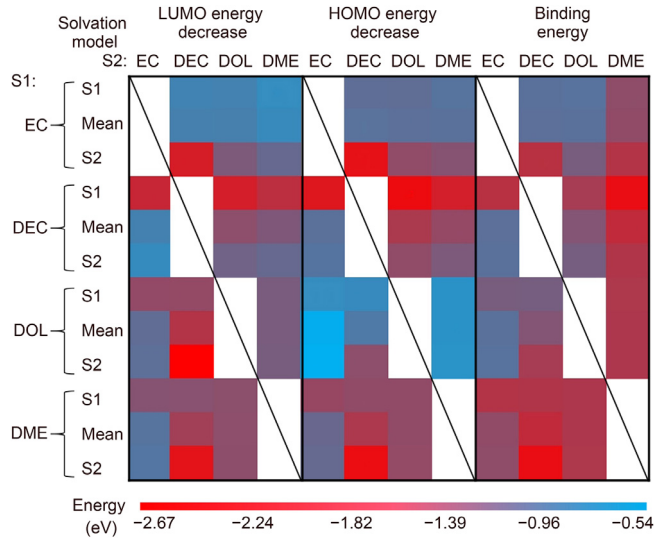

Fig. 4. Color map depicting the decrease in HOMO energy, decrease in LUMO energy, and the binding energy of binary-solvent complexes (Li^+–S1–S2). S1 and S2 represent the first and the second solvents in the complex, respectively. The solvation models "S1," "Mean," and "S2" represent the parameters of the first solvent, the average parameters of the two solvents, and the parameters of the second solvent, respectively. They are used to model the solvation environment of complexes.

ether solvents [48]. In comparison with linear ester DEC, cyclic ester EC presents more obvious changes in both the HOMO and LUMO energies, which explains why EC is preferred by lithium ions in EC–DEC mixtures.

The fruitful results from binary-solvent complexes are insightful for exploring new electrolytes. First, the interaction strength between Li ions and solvents is determined by both the solvent and electrolyte solvation environment. Solvents with a large binding energy towards a Li ion are generally preferred in the solvation shell, but they impede the rapid desolvation at the electrolyte–electrode interface, which largely determines the low-temperature and rate performances rates of LBs. Non-solvating solvents that can weaken Li^+–solvent and Li^+–anion interactions are promising in this regard. Second, the formation of ion–solvent complexes is supposed to illustrate the chemical origin of the instability of organic electrolytes on lithium metal anodes. Molecular designs to enhance the intrinsic stability or to induce a stable solid electrolyte interphase have been widely considered [49–54]. Simultaneously, it is of equal importance to regulate the electrolyte solvation environment, which also has a vital influence on the stability of the solvents in solvation shells. Third, the redox stability of solvents in lithium-ion solvation shells is more important for the electrolyte design, as free and coordinated solvents can exhibit different trends of redox stability. Constructing a large dataset of ion–solvent complexes will promote the rational design of electrolytes for building high-energy-density lithium batteries.

4. Conclusions

In conclusion, ion–solvent chemistry was developed from mono-solvent to multi-solvent complexes. The decrease in both the HOMO and LUMO energies becomes less significant with an increase in the number of coordinated solvents in the solvation shell of lithium ions. A positive and approximately linear relationship is found between the decrease in both the HOMO and LUMO energies and the average binding energy, from which the ion–solvent interactions in multi-solvent complexes can be well understood. The exploration of binary-solvent complexes highlights the importance of the solvation environment in the regulation of electrolyte stability. In addition, free and coordinated solvents can exhibit different trends in both HOMO and LUMO energies, demonstrating the crucial role of the ion–solvent model in probing electrolyte stability. Combined with a large dataset obtained from ion–solvent complexes and machine learning methods, it is highly expected that ion–solvent chemistry can accelerate the high-throughput design of advanced electrolytes for the building of next-generation lithium batteries as well as other rechargeable battery systems.

Declaration of Competing Interest

The authors declared that they have no conflict of interest to this work.

Acknowledgments

This work was supported by the National Natural Science Foundation of China (21825501), Beijing Municipal Natural Science Foundation (Z20J00043), National Key Research and Development Program (2016YFA0200102), and Grant 2020GQG1006 from the Guoqiang Institute at Tsinghua University. X. Chen appreciates the support from the Shuimu Tsinghua Scholar Program of Tsinghua University and the Project funded by China Postdoctoral Science Foundation (2021TQ0161 and 2021M691709). The authors acknowledged the support from Tsinghua National Laboratory for Information Science and Technology for theoretical simulations.

Supplementary materials

Supplementary material associated with this article can be found, in the online version, at doi:10.1016/j.fmre.2021.06.011.

References

[1] X.-B. Cheng, R. Zhang, C.-Z. Zhao, et al., Toward safe lithium metal anode in rechargeable batteries: a review, Chem. Rev. 117 (2017) 10403–10473.
[2] J.W. Choi, D. Aurbach, Promise and reality of post-lithium-ion batteries with high energy densities, Nat. Rev. Mater. 1 (2016) 16013.
[3] D. Larcher, J.M. Tarascon, Towards greener and more sustainable batteries for electrical energy storage, Nat. Chem. 7 (2015) 19–29.
[4] J. Liu, Z. Bao, Y. Cui, et al., Pathways for practical high-energy long-cycling lithium metal batteries, Nat. Energy 4 (2019) 180–186.
[5] S. Chu, Y. Cui, N. Liu, The path towards sustainable energy, Nat. Mater. 16 (2017) 16–22.
[6] X. Chen, T. Hou, K.A. Persson, et al., Combining theory and experiment in lithium—sulfur batteries: current progress and future perspectives, Mater. Today 22 (2019) 142–158.
[7] A. Gupta, A. Manthiram, Designing advanced lithium-based batteries for low-temperature conditions, Adv. Energy Mater. 10 (2020) 2001972.
[8] Y. Liu, Y. Zhu, Y. Cui, Challenges and opportunities towards fast-charging battery materials, Nat. Energy 4 (2019) 540–550.
[9] G. Harper, R. Sommerville, E. Kendrick, et al., Recycling lithium-ion batteries from electric vehicles, Nature 575 (2019) 75–86.
[10] M.-T.F. Rodrigues, G. Babu, H. Gullapalli, et al., A materials perspective on Li-ion batteries at extreme temperatures, Nat. Energy 2 (2017) 17108.
[11] X. Chen, Q. Zhang, Atomic insights into the fundamental interactions in lithium battery electrolytes, Acc. Chem. Res. 53 (2020) 1992–2002.
[12] Y. Yamada, J. Wang, S. Ko, et al., Advances and issues in developing salt-concentrated battery electrolytes, Nat. Energy 4 (2019) 269–280.
[13] K. Xu, Electrolytes and interphases in Li-ion batteries and beyond, Chem. Rev. 114 (2014) 11503–11618.
[14] J.-G. Zhang, W. Xu, J. Xiao, et al., Lithium metal anodes with nonaqueous electrolytes, Chem. Rev. 120 (2020) 13312–13348.
[15] J.-F. Ding, R. Xu, C. Yan, et al., A review on the failure and regulation of solid electrolyte interphase in lithium batteries, J. Energy Chem. 59 (2021) 306–319.
[16] X. Chen, T.-Z. Hou, B. Li, et al., Towards stable lithium–sulfur batteries: mechanistic insights into electrolyte decomposition on lithium metal anode, Energy Storage Mater. 8 (2017) 194–201.
[17] P. Zhai, L. Liu, X. Gu, et al., Interface engineering for lithium metal anodes in liquid electrolyte, Adv. Energy Mater. 10 (2020) 2001257.
[18] S. Li, M. Jiang, Y. Xie, et al., Developing high-performance lithium metal anode in liquid electrolytes: Challenges and progress, Adv. Mater. 30 (2018) 1706375.
[19] H. Yang, J. Li, Z. Sun, et al., Reliable liquid electrolytes for lithium metal batteries, Energy Storage Mater. 30 (2020) 113–129.
[20] H. Zhang, G.G. Eshetu, X. Judez, et al., Electrolyte additives for lithium metal anodes and rechargeable lithium metal batteries: progress and perspectives, Angew. Chem. Int. Ed. 57 (2018) 15002–15027.
[21] G. Xu, X. Shangguan, S. Dong, et al., Key scientific issues in formulating blended lithium salts electrolyte for lithium batteries, Angew. Chem. Int. Ed. 59 (2020) 3400–3415.

[22] L. Kong, L. Yin, F. Xu, et al., Electrolyte solvation chemistry for lithium–sulfur batteries with electrolyte-lean conditions, J. Energy Chem. 55 (2021) 80–91.
[23] X. Chen, X. Shen, B. Li, et al., Ion-solvent complexes promote gas evolution from electrolytes on a sodium metal anode, Angew. Chem. Int. Ed. 57 (2018) 734–737.
[24] X. Chen, H.-R. Li, X. Shen, et al., The origin of the reduced reductive stability of ion–solvent complexes on alkali and alkaline earth metal anodes, Angew. Chem. Int. Ed. 57 (2018) 16643–16647.
[25] X. Chen, Y.-K. Bai, C.-Z. Zhao, et al., Lithium bonds in lithium batteries, Angew. Chem. Int. Ed. 59 (2020) 11192–11195.
[26] X. Chen, X. Shen, T.-Z. Hou, et al., Ion-solvent chemistry-inspired cation-additive strategy to stabilize electrolytes for sodium-metal batteries, Chem 6 (2020) 2242–2256.
[27] S. Plimpton, Fast parallel algorithms for short-range molecular dynamics, J. Comput. Phys. 117 (1995) 1–19.
[28] L.S. Dodda, I. Cabeza de Vaca, J. Tirado-Rives, et al., Ligpargen web server: an automatic opls-aa parameter generator for organic ligands, Nucleic. Acids. Res. 45 (2017) W331–W336.
[29] T. Lu, F. Chen, Multiwfn: A multifunctional wavefunction analyzer, J. Comput. Chem. 33 (2012) 580–592.
[30] K.P. Jensen, W.L. Jorgensen, Halide, ammonium, and alkali metal ion parameters for modeling aqueous solutions, J. Chem. Theory Comput. 2 (2006) 1499–1509.
[31] B. Doherty, X. Zhong, S. Gathiaka, et al., Revisiting opls force field parameters for ionic liquid simulations, J. Chem. Theory Comput. 13 (2017) 6131–6145.
[32] M. Parrinello, A. Rahman, Polymorphic transitions in single crystals: a new molecular dynamics method, J. Appl. Phys. 52 (1981) 7182–7190.
[33] W.G. Hoover, Canonical dynamics: equilibrium phase-space distributions, Phys. Rev. A 31 (1985) 1695–1697.
[34] S. Nosé, A molecular dynamics method for simulations in the canonical ensemble, Mol. Phys. 52 (1984) 255–268.
[35] M. J. Frisch, G.-W. Trucks, H. B. Schlegel, et al., Gaussian 09, revision b. 01, Gaussian Inc., Wallingford, CT (2010).
[36] A.-D. Becke, Density-functional thermochemistry. III. The role of exact exchange, J. Chem. Phys. 98 (1993) 5648–5652.
[37] A.V. Marenich, C.J. Cramer, D.G. Truhlar, Universal solvation model based on solute electron density and on a continuum model of the solvent defined by the bulk dielectric constant and atomic surface tensions, J. Phys. Chem. B 113 (2009) 6378–6396.
[38] Jr B.H. Besler, K.M. Merz, P.A. Kollman, Atomic charges derived from semiempirical methods, J. Comput. Chem. 11 (1990) 431–439.
[39] U.C. Singh, P.A. Kollman, An approach to computing electrostatic charges for molecules, J. Comput. Chem. 5 (1984) 129–145.
[40] X. Chen, X.-Q. Zhang, H.-R. Li, et al., Cation–solvent, cation–anion, and solvent–solvent interactions with electrolyte solvation in lithium batteries, Batteries Supercaps 2 (2019) 128–131.
[41] J. Self, K.D. Fong, K.A. Persson, Transport in superconcentrated $LiPF_6$ and $LiBF_4$/propylene carbonate electrolytes, ACS Energy Lett. 4 (2019) 2843–2849.
[42] J. Qian, W.A. Henderson, W. Xu, et al., High rate and stable cycling of lithium metal anode, Nat. Commun. 6 (2015) 6362.
[43] X. Ren, S. Chen, H. Lee, et al., Localized high-concentration sulfone electrolytes for high-efficiency lithium-metal batteries, Chem 4 (2018) 1877–1892.
[44] K. Xu, Nonaqueous liquid electrolytes for lithium-based rechargeable batteries, Chem. Rev. 104 (2004) 4303–4417.
[45] W.-J. Chen, B.-Q. Li, C.-X. Zhao, et al., Electrolyte regulation towards stable lithium metal anode in lithium–sulfur batteries with sulfurized polyacrylonitrile cathode, Angew. Chem. Int. Ed. 59 (2020) 10732–10745.
[46] M. Zhao, B.-Q. Li, H.-J. Peng, et al., Challenges and opportunities towards practical lithium–sulfur batteries under lean electrolyte conditions, Angew. Chem. Int. Ed. 59 (2020) 12636–12652.
[47] Q. Pang, X. Liang, C.Y. Kwok, et al., Advances in lithium–sulfur batteries based on multifunctional cathodes and electrolytes, Nat. Energy 1 (2016) 16132.
[48] Y.-X. Yao, X. Chen, C. Yan, et al., Regulating interfacial chemistry in lithium-ion batteries by a weakly-solvating electrolyte, Angew. Chem. Int. Ed. 60 (2020) 4090–4097.
[49] X.-Q. Zhang, X. Chen, L.-P. Hou, et al., Regulating anions in the solvation sheath of lithium ions for stable lithium metal batteries, ACS Energy Lett. 4 (2019) 411–416.
[50] X.-Q. Zhang, X.-B. Cheng, X. Chen, et al., Fluoroethylene carbonate additives to render uniform Li deposits in lithium metal batteries, Adv. Funct. Mater. 27 (2017) 1605989.
[51] Z. Yu, H. Wang, X. Kong, et al., Molecular design for electrolyte solvents enabling energy-dense and long-cycling lithium metal batteries, Nat. Energy 5 (2020) 526–533.
[52] X. Fan, X. Ji, L. Chen, et al., All-temperature batteries enabled by fluorinated electrolytes with non-polar solvents, Nat. Energy 4 (2019) 882–890.
[53] J. Chen, X. Fan, Q. Li, et al., Electrolyte design for lif-rich solid–electrolyte interfaces to enable high-performance microsized alloy anodes for batteries, Nat. Energy 5 (2020) 386–397.
[54] J. Chen, T. Liu, L. Gao, et al., Tuning the solution structure of electrolyte for optimal solid-electrolyte-interphase formation in high-voltage lithium metal batteries, J. Energy Chem. 60 (2021) 178–185.

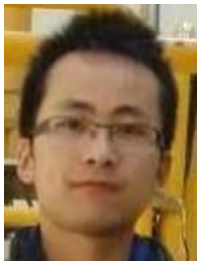

Xiang Chen gained his Bachelor's and Ph.D. degree from the Department of Chemical Engineering at Tsinghua University in 2016 and 2021, respectively. He is currently a postdoctoral fellow at Tsinghua University. His research interests focus on understanding the chemical mechanism and materials science in rechargeable batteries.

Qiang Zhang received his Bachelor's and Ph.D. degrees from Tsinghua University in 2004 and 2009, respectively. After a stay at Case Western Reserve University in the USA and the Fritz Haber Institute of the Max Planck Society in Germany, he joined Tsinghua University in 2011. He held the Newton Advanced Fellowship from the Royal Society and the National Science Fund for Distinguished Young Scholars. His current research interests are advanced energy materials, including Li metal anodes, solid-state electrolytes, Li–S batteries, and electrocatalysts.